3.45–4.25 (m, 15 H, H(1')/H(2')/$POCH_2$). ^{13}C NMR (C_6D_5Br): δ 26.0 (C(2')), 28.3 (C(3')), 64.7 (C(4')), 68.3 (C(1')), 78.2 ($POCH_2$). ^{31}P NMR ($CDCl_3$): δ 139.0.

Tris(cyclopentylmethyl) Phosphite. To a stirred and cooled (0 °C) solution of cyclopentylmethyl alcohol (40.8 g; 408 mmol) and triethylamine (41.2 g; 408 mmol) in 600 mL of anhydrous diethyl ether was added dropwise a solution of PCl_3 (18.7 g; 136 mmol) in 100 mL of anhydrous diethyl ether. After completion of the addition, the mixture was stirred for 0.5 h at room temperature and refluxed for 1 h. The precipitated triethylamine hydrochloride was removed by filtration. After removal of the solvent the oily residue was distilled under reduced pressure affording the desired product as a colorless liquid. Bp: 148 °C (0.01 mmHg). Yield: 62%. ^1H NMR ($CDCl_3$): δ 1.30–1.85 (m, 27 H, H(1')/H(2')/H(3')/H(4')/X), 3.70 (t, 6 H, $POCH_2$). ^{13}C NMR (C_6D_5Br): δ 25.7 (C(1')/C(2')), 29.5 (C(3')/X), 41.0 (C(4')), 66.0 ($POCH_2$). ^{31}P NMR ($CDCl_3$): 139.1.

Tris(2-methoxyethyl) Phosphite. This compound was prepared from 2-methoxyethanol and PCl_3 according to the procedure described for the preparation of tris(cyclopentylmethyl) phosphite. Bp: 83 °C (0.25 mmHg). Yield: 65%. ^1H NMR ($C_6D_5CD_3$): δ 3.25 (s, 3 H, OCH_3), 3.43 (t, 2 H, OCH_2), 3.96 (dt, 2 H, $POCH_2$). ^{13}C NMR ($C_6D_5CD_3$): δ 58.5 (OCH_3), 61.5 ($POCH_2$), 72.6 (OCH_2). ^{31}P NMR ($C_6D_5CD_3$): δ 139.8.

3-(Phenylmethylene)-2,4-pentanedione was prepared from benzaldehyde and 2,4-pentanedione according to a literature procedure.[24] Bp: 168–170 °C (13 mmHg). Yield: 73%. ^1H NMR ($CDCl_3$): δ 2.23 (s, 3 H, $COCH_3$), 2.38 (s, 3 H, $COCH_3$), 7.27 (m, 5 H, Ar), 7.37 (s, 1 H, CH). ^{13}C NMR (CD_2Cl_2): δ 25.5 ($COCH_3$), 30.9 ($COCH_3$), 128.3–130.0 (phenyl), 132.5 (ipso), 138.9 (C=C), 144.9 (C=C), 200.4 (C=O). Anal. Calcd for $C_{12}H_{12}O_2$: C, 76.57; H, 6.43. Found: C, 77.05; H, 6.53. MS, *m/e* 188.15 (M^+; calcd 188.23).

3-(1-Methylethylidene)-2,4-pentanedione was prepared from 2-chloro-2-nitropropane and 2,4-pentanedione according to a procedure described by Russell et al.[25] Bp: 60–80 °C (8 mmHg). Yield: 23%. ^1H NMR ($CDCl_3$): δ 1.96 (s, 6 H, $COCH_3$), 2.29 (s, 6 H, $C(CH_3)_2$). ^{13}C NMR (CD_3COCD_3): δ 23.9 ($C(CH_3)_2$), 32.3 ($COCH_3$), 143.5 (C=C), 148.4 (C=C), 201.8 (C=O). Anal. Calcd for $C_8H_{12}O_2$: C, 68.55; H, 8.63. Found: C, 67.92; H, 8.81. MS, *m/e* 140.20 (M^+; calcd 140.18).

Ethyl α-Isopropylideneacetoacetate. This compound was prepared from 2-chloro-2-nitropropane and ethyl acetoacetate according to the procedure described for the preparation of 3-(1-methylethylidene)-2,4-pentanedione. Bp: 87–88 °C (6 mmHg). Yield: 39%. ^1H NMR ($CDCl_3$): δ 1.30 (t, 3 H, CH_3), 1.97 (s, 3 H, $COCH_3$), 2.10 (s, 3 H, $C(CH_3)$), 2.30 (s, 3 H, $C(CH_3)$), 4.25 (q, 2 H, OCH_2). ^{13}C NMR ($C_6D_5CD_3$): δ 15.5 (CH_3), 24.1 ($C(CH_3)_2$), 31.5 ($COCH_3$), 61.8 (OCH_2), 134.1 (C=C), 153.4 (C=C), 167.1 (C=O), 200.3 (C=O). Anal. Calcd for $C_9H_{14}O_3$: C, 63.51; H, 8.29. Found: C, 64.09; H, 8.23. MS, *m/e* 170.15 (M^+; calcd 170.21).

Pentacoordinated Phosphorus Compounds. In order to avoid decomposition during handling and purification of the phosphoranes, they were prepared in situ in the NMR tubes by adding equivalent amounts of freshly distilled phosphite and the selected pentanedione to the deuteriated solvents. The tubes were flushed with dry Argon and sealed. After leaving them at room temperature for 10–14 days, ^{31}P NMR indicated the reactions to be complete. ^1H, ^{13}C, and ^{31}P NMR spectra were then recorded and are listed in Tables I and II (vide supra).

Line-Shape Analysis. The rate constant *k* was obtained for each temperature by simulation of the experimental spectrum. Analyzing the coupled two-site exchange patterns (with $J_{AB} = 0$), using the DNMR/3 program,[10] the simulated spectra for all the different temperatures were obtained. For each study at least nine different temperatures were used. The $\Delta G^{\ddagger}$ was obtained from a least-squares plot of ln (k/T) versus $1/T$, using the Eyring model. The calculated errors lie within ±0.5 kJ·mol^{-1}. The validity of the $\Delta G^{\ddagger}$ values has been tested by calculating them from the equation $\Delta G^{\ddagger} = 1.91 \times 10^{-2} T_c(9.973 + \log (T_c/\Delta\nu))$. An excellent agreement with the values obtained from the line-shape analysis was found (Table III, vide supra).

Acknowledgment. This investigation has been supported by the Netherlands Foundation for Chemical Research (SON) with financial aid from the Netherlands Organization for the Advancement of Pure Research (ZWO). We thank Dr. N. K. de Vries for recording the ^{13}C NMR spectra of compound **a**[7] and Dr. P. A. Leclercq for recording the mass spectra of the pentadiones.

Registry No. 1, 1091-15-2; **2a**, 115094-83-2; **2b**, 115094-86-5; **2c**, 115094-84-3; **2d**, 115117-26-5; **3a**, 115094-85-4; **3b**, 115094-87-6; **3c**, 115117-25-4; **3d**, 115094-88-7; PCl_3, 7719-12-2; cyclopentylmethyl alcohol, 3637-61-4; 2-methoxyethanol, 109-86-4; 3-(phenylmethylene)-2,4-pentanedione, 4335-90-4; 3-(1-methylethylidene)-2,4-pentanedione, 26187-41-7; ethyl α-isopropylideneacetoacetate, 35044-52-1; 2-chloro-2-nitropropane, 594-71-8; ethyl acetoacetate, 141-97-9; tris(tetrahydrofurfuryl) phosphite, 5971-30-2; tris(cyclopentylmethyl) phosphite, 115094-89-8; tris(2-methoxyethyl) phosphite, 4156-80-3.

(24) McEntee, M. E.; Pinder, A. R. *J. Chem. Soc.* **1957**, 4426.
(25) Russell, G. A.; Mudryk, B.; Jawdosiuk, M. *Synthesis* **1981**, 62.

A Single-Crystal ESR Study on Radicals Derived from *rac*- and *meso*-1,2-Dimethyl-1,2-diphenyldiphosphine Disulfide: Stereochemical Selection in Radical Formation

René A. J. Janssen,* Mark J. van der Woerd, Olav M. Aagaard, and Henk M. Buck

Contribution from the Department of Organic Chemistry, Eindhoven University of Technology, P.O. Box 513, 5600 MB Eindhoven, The Netherlands. *Received November 23, 1987*

Abstract: An ESR study on electron-capture phosphorus centered radicals trapped in single crystals of *rac*- and *meso*-1,2-dimethyl-1,2-diphenyldiphosphine disulfide (MePhP(S)P(S)MePh) is reported. The principal values and axes of the **g** and hyperfine coupling tensors of the radical anions are determined. It is shown that X irradiation of the two diastereoisomeric compounds results in completely different radical products. The racemate yields a radical product in which the extra electron is symmetrically distributed over the two phosphorus nuclei, whereas for the meso form exclusively asymmetric electronic configurations are detected.

For many years the formation and structure of free radicals, produced by ionizing radiation, has received much attention. Numerous ESR experiments have been performed to elucidate the principles that determine the electronic structure and molecular geometry of the formed doublet species. This has resulted in a detailed understanding of the role of the nucleus at the radical center and of the influence of the surrounding ligands. Stereochemical aspects, however, are not generally included in these analyses. In the present study we report the formation of phosphorus-centered radicals in single crystals of racemic (*R*,*R* and

0002-7863/88/1510-6001$01.50/0

S,S) and meso (R,S) 1,2-dimethyl-1,2-diphenyldiphosphine disulfide.

The molecular conformation of diphosphine disulfides in the solid state is characterized by a trans orientation of the two sulfur nuclei:[1]

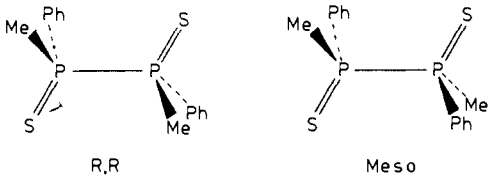

In a recent study on X-irradiated tetrasubstituted diphosphine disulfides ($R_2P(S)P(S)R_2$), also possessing a trans orientation, we showed that the radiation process invariably results in the formation of an electron-capture radical product in which the unpaired electron occupies an antibonding orbital between the two phosphorus nuclei, resulting in a three-electron bond.[2] This structure, which has been established by both single-crystal ESR and ab initio quantum chemical methods, possesses a symmetrical distribution of the unpaired electron:

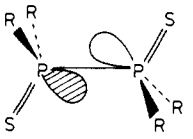

Depending on the nature of the substituents several other primary and secondary radical configurations were also identified. We will now show that the two diastereoisomeric forms of the title compound give rise to completely different radical products upon X irradiation. The radiation process of the racemate involves the formation of a symmetric species with a three-electron P–P bond as described above. The meso form, on the other hand, yields exclusively asymmetric radical configurations in which the unpaired electron is mainly localized on one of the two phosphorus nuclei. The electronic structure of these radicals as determined by an interpretation of the experimental single-crystal ESR results is presented and compared with theoretical calculations.

Experimental Section

Synthesis. 1,2-Dimethyl-1,2-diphenyldiphosphine disulfide was synthesized from dichlorophenylphosphine sulfide and methylmagnesium iodide following a procedure analogous to the one described by Maier.[3] The two diastereoisomeric forms were easily separated by extraction of the crude reaction product with ethanol. The meso form, unsoluble in ethanol, was collected by filtration and recrystallized twice from chloroform. Single crystals of the meso form were prepared by slow evaporation of a chloroform solution in a stream of dry nitrogen. The racemic form was recrystallized several times from ethanol. Slow evaporation of an ethanolic solution of the racemate afforded needle-shaped crystals. Larger plate-shaped single crystals, more suitable for ESR experiments, were obtained from a slow evaporation of a pentane solution. Meso: ^{1}H NMR ($CDCl_3$) δ 1.97 (m, 3, CH_3), 7.58 (m, 3, PhH), 8.13 (m, 2, PhH); ^{31}P NMR ($CDCl_3$) δ 36.55; MS, *m/e* (rel intensity) 311 (93), 279 (6), 157 (100), 125 (48); mp 202 °C. Racemate: ^{1}H NMR ($CDCl_3$) δ 2.46 (m, 3, CH_3), 7.18–7.63 (m, 5, PhH); ^{31}P NMR ($CDCl_3$) δ 37.62; MS, *m/e* (rel intensity) 311 (11), 279 (11), 157 (100), 125 (42); mp 144 °C.

Irradiation and ESR. Single crystals of *rac*- and *meso*-1,2-dimethyl-1,2-diphenyldiphosphine disulfide were mounted on a quartz rod and subsequently sealed in a quartz tube. The crystals were X-irradiated in a glass Dewar vessel containing liquid nitrogen (77 K) with unfiltered radiation from a Cu source operating at 40 KV and 20 mA for 6 h. ESR experiments were performed with a Bruker ER200D spectrometer interfaced with a Bruker Aspect 3000 computer and operating with a X-band standard cavity. Microwave power was set as low as possible, being 2 mW in most experiments. The crystals were rotated perpendicular to the magnetic field with a single-axis goniometer in 10° steps.

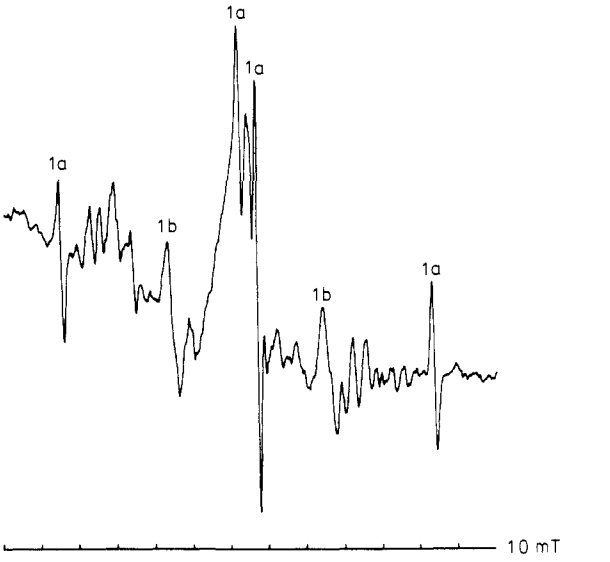

Figure 1. Single-crystal ESR spectrum of X-irradiated *rac*-1,2-dimethyl-1,2-diphenyldiphosphine disulfide at 105 K showing the features of radicals **1a** and **1b**.

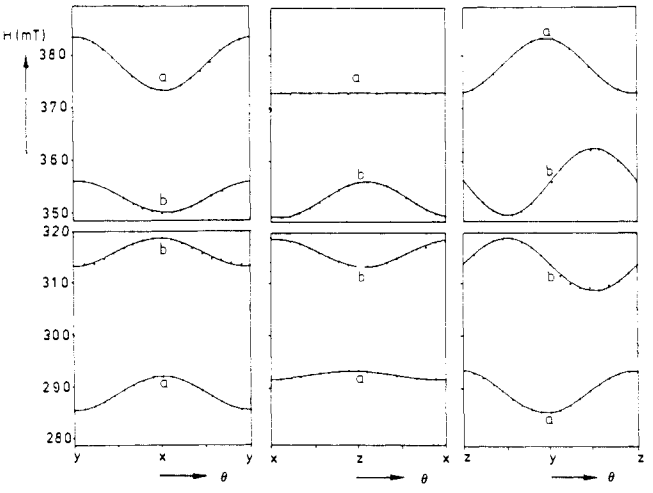

Figure 2. Angular dependence of the ESR signals due to radicals **1a** and **1b**.

Temperature was controlled with the aid of a variable-temperature unit operating between 90 K and room temperature. ESR parameters were obtained from a second-order analysis of the spectra.

Results and Assignment

***rac*-1,2-Dimethyl-1,2-diphenyldiphosphine Disulfide (1).** Although there is no conclusive description of the crystal structure of *rac*-1,2-dimethyl-1,2-diphenyldiphosphine disulfide (**1**) it is known that the racemate crystallizes in the triclinic space group $P\bar{1}$ with two molecules (*R,R* and *S,S*) in the unit cell, centrosymmetrically related to each other.[4] After X irradiation of a single crystal of the racemate at 77 K the ESR spectrum recorded at 105 K shows the weak transitions of at least two different radical species (Figure 1).[5] The outermost features can be assigned to the $m_I = 1$ and $m_I = -1$ absorptions of a radical with a hyperfine coupling to two indentical phosphorus nuclei (radical **1a**). The large phosphorus hyperfine interaction results in a pronounced splitting between the two central $m_I = 0$ lines, due to the nondegenaracy of the $I = 1$, $m_I = 0$ and $I = 0$, $m_I = 0$ energy levels (second-order splitting).[6,7] The second radical product (**1b**)

(1) Harris, R. K.; Merwin, L. H.; Hägele, G. *J. Chem. Soc., Faraday Trans. 1* **1987**, *83*, 1055.
(2) Janssen, R. A. J.; Sonnemans, M. H. W.; Buck, H. M. *J. Chem. Phys.* **1986**, *84*, 3694.
(3) Maier, L. *Chem. Ber.* **1961**, *94*, 3043.
(4) Wheatley, P. J. *J. Chem. Soc.* **1960**, 523.
(5) The ESR spectra of Figures 1 and 4 were obtained from randomly oriented single crystals that were transferred after the X irradiation at 77 K to an unirradiated sample tube in order to remove the overlapping central absorptions due to the irradiated quartz.
(6) Fessenden, R. W. *J. Chem. Phys.* **1962**, *37*, 747.

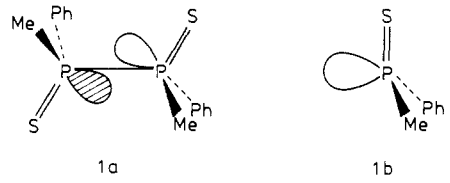

1a 1b

Figure 3. Structure of radicals **1a** and **1b**.

Table I. Hyperfine Tensors of Radicals **1a** and **1b** in *rac*-1,2-Dimethyl-1,2-diphenyldiphosphine Disulfide

radical	total tensor (MHz)	isotropic (MHz)	dipolar (MHz)	direction cosines		
				x	*y*	*z*
1a	1122	1213	−91	−0.013	0.078	0.997
	1143		−70	0.990	−0.136	0.024
	1374		161	0.137	0.988	0.075
1b	803	1042	−239	−0.311	0.668	−0.676
	867		−175	0.950	0.250	−0.189
	1456		414	−0.043	0.701	0.712

Table II. g Tensors of Radicals **1a** and **1b**

radical	g	direction cosines		
		x	*y*	*z*
1a	1.994	0.005	0.990	−0.140
	2.007	0.087	0.139	0.986
	2.012	0.996	−0.018	−0.086
1b	1.996	−0.085	0.655	0.751
	2.012	0.921	−0.236	0.310
	2.013	0.380	0.718	−0.583

exhibits hyperfine interaction of the unpaired electron with a single phosphorus nucleus.

For all orientations of the single crystal with respect to the magnetic field direction only a single spectrum of the two radicals **1a** and **1b** is observed. This absence of site splitting is in accordance with the presence of a center of symmetry in the unit cell which results in a coalignment of the S–P–P–S linkages of the *R,R* and *S,S* molecules. A complete single-crystal analysis was obtained by rotating the crystal in three mutual orthogonal planes (Figure 2). For that purpose one of the ESR reference axes (x) was chosen perpendicular to the plate face, the remaining two (y, z) were directed parallel to the extinction directions in the plate face with use of a polarization microscope. A central absorption due to the irradiated quartz tube prevented the observation of the two $m_I = 0$ transitions for all orientations of the single crystal. For this reason the hyperfine coupling and g factor of radical **1a** were evaluated from the $m_I = \pm 1$ lines, and when possible checked with the $m_I = 0$ position(s). The principal values and direction cosines of the A and **g** tensors of radicals **1a** and **1b** are compiled in Tables I and II. It appears that for both species the direction of the maximum A value (A_{zz}) is close to that of the minimum g value. This is expected because it is the direction of the phosphorus 3p orbital contributing to the singly occupied molecular orbital (SOMO).

Radical **1a** is attributed to a three-electron-bond radical (Figure 3), based on the hyperfine coupling to two identical phosphorus nuclei and the values of $A^{iso} = 1213$ MHz ($A^{iso} = {}^1/_3(A_{xx} + A_{yy} + A_{zz})$ and $B_{zz} = 161$ MHz ($B_{zz} = A_{zz} - A^{iso}$), which are close to the corresponding values of three-electron-bond radicals in X-irradiated tetramethyl-, tetraethyl-, and tetraphenyldiphosphine disulfides ($1224 < A^{iso} < 1395$ MHz, $155 < B_{zz} < 173$ MHz).[2] The values of the isotropic (A^{iso}) and dipolar (B_{zz}) hyperfine couplings are commonly interpreted in terms of atomic valence s and p orbital contributions to the SOMO by comparing the experimental couplings to a set of calculated values for the free atom. This analysis, using the atomic parameters compiled by Morton and Preston,[8] results in $\rho_{3s} = 9.1\%$ and $\rho_{3p} = 21.9\%$ (p/s = 2.4) for each phosphorus nucleus of **1a**.

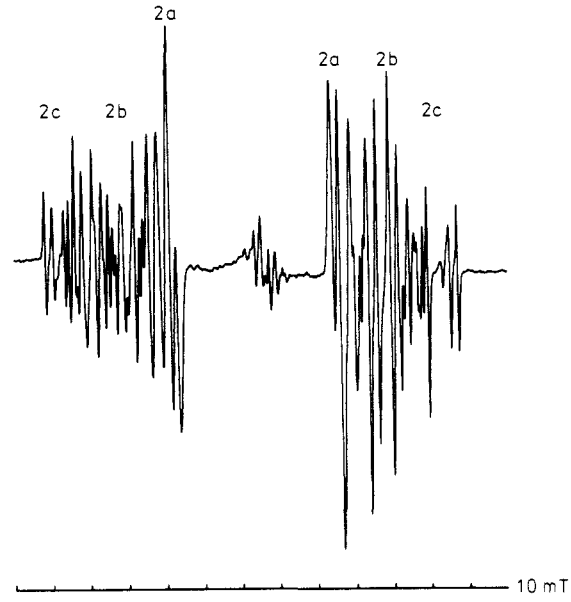

Figure 4. Single-crystal ESR spectrum of X-irradiated *meso*-1,2-dimethyl-1,2-diphenyldiphosphine disulfide at 105 K.

Radical **1b**, exhibiting hyperfine coupling to one phosphorus nucleus, is assigned to a dissociation product resulting from a rupture of the P–P linkage (Figure 3). The estimated spin densities $\rho_{3s} = 7.8\%$ and $\rho_{3p} = 56.3\%$ and the resulting p/s ratio of 7.2 indicate a large contribution of the phosphorus $3p_z$ orbital and a considerable flattening of the original tetrahedral geometry. The experimental hyperfine couplings of **1b** are in close agreement with those observed for $Ph_2\dot{P}S$ formed in diphenylphosphine sulfide[9] and with the values of $Et_2\dot{P}S$ in X-irradiated tetraethyldiphosphine disulfide.[2]

The spectrum of radical **1a** is irreversibly lost upon annealing above 135 K. Further warming results in the loss of **1b** at approximately 170 K.

***meso*-1,2-Dimethyl-1,2-diphenyldiphosphine Disulfide (2).** The meso form of 1,2-dimethyl-1,2-diphenyldiphosphine disulfide crystallizes as lozenge-like crystals in the orthorhombic space group *Pbca* with unit cell parameters $a = 17.10$ Å, $b = 10.62$ Å and $c = 8.59$ Å.[4] The four molecules in the unit cell lie on a center of symmetry and are all differently oriented with respect to the crystallographic axes. The ESR spectrum of an X-irradiated single crystal of **2**, recorded at 105 K (Figure 4), exhibits a few low-intensity transitions in the central region and strong absorptions in the lateral region. The large splitting between the two groups of signals undoubtly results from the interaction of the unpaired electron with a phosphorus nucleus. An important difference between the spectra of the meso (Figure 4) and the racemic form (Figure 1) is the absence of two $m_I = 0$ transitions in the $g = 2$ region for the first. From this it can unambiguously be concluded that X-irradiation of the meso form, unlike the racemic form, does not result in the formation of a three-electron-bond radical with a symmetrical electron density distribution over the two phosphorus nuclei.

In order to obtain a more detailed analysis of the ESR spectrum, a single crystal of the meso form was rotated in three mutual orthogonal planes. The ESR reference axes were chosen as follows; the z axis points perpendicular from the plate face and the x and y axes coincide with the extinction directions of the crystal in the plate face. Rotation of the crystal in the xy, xz, yz planes reveals the presence of two sites, symmetrically related to each other. The spectra of the two sites coalesce when the x, y, or z axis is parallel to the external magnetic field direction. In fact, there are four sites corresponding to the four molecules in the unit cell which reduce to two in a crystallographic plane (xy, xz, or yz) and to one site along a crystallographic axis (x, y, or z). Since there is

(7) Fessenden, R. W.; Schuler, R. H. *J. Chem. Phys.* **1965**, *43*, 2704.
(8) Morton, J. R.; Preston, K. F. *J. Magn. Reson.* **1978**, *30*, 577.
(9) Geoffroy, M. *Helv. Chim. Acta* **1973**, *56*, 1552.

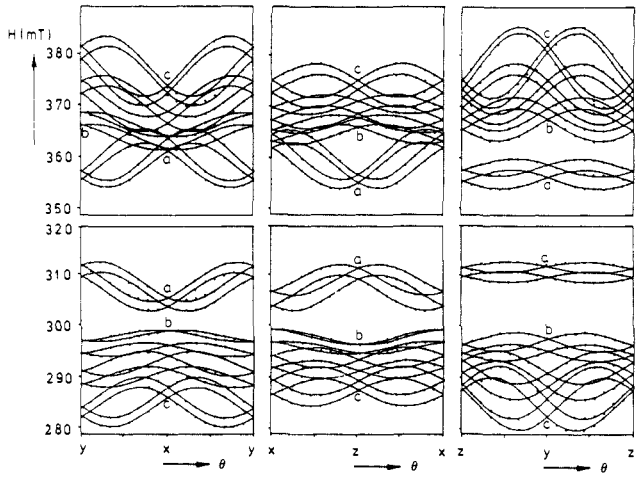

Figure 5. Angular dependence of the ESR signals due to radicals **2a**, **2b**, and **2c**.

Table III. Hyperfine Tensors of Radicals **1a**, **2b**, and **2c** in *meso*-1,2-Dimethyl-1,2-diphenyldiphosphine Disulfide

radical	total tensor (MHz)	isotropic (MHz)	dipolar (MHz)	direction cosines		
				x	y	z
2a	1201	1379	−178	−0.105	0.775	0.624
	1231		−148	0.465	−0.516	0.719
	1705		326	0.879	0.365	−0.306
2b	1826	1934	−108	0.978	−0.203	0.057
	1856		−78	0.099	0.683	0.723
	2120		186	0.186	0.701	−0.688
2c	2103	2316	−213	0.371	0.357	0.857
	2156		−160	0.844	−0.514	−0.152
	2689		373	0.387	0.780	−0.492
	81	139	−58	0.167	0.278	0.946
	114		−25	0.829	−0.559	0.018
	222		83	0.533	0.781	−0.324

a large number of signals, which are frequently overlapping, the elucidation of the angular variation of the hyperfine lines was not straightforward. For this reason the low and high field curves were determined as the best fit of a quadratic sine to the experimental magnetic field values, using a least-squares regression analysis. The resulting angular variation of the signals is presented in Figure 5. Going from one rotation experiment to another, there is an ambiguity in the relation between the curves in the two series. This ambiguity results in four possible assignments that are just the four orientations of the same radical in the crystal.

The ESR spectra of the X-irradiated meso form and the angular variation can be interpreted by assuming the presence of at least four different phosphorus-centered radicals. For three species a clear angular variation is observed; a fourth was undoubtly present but could not be analyzed in detail. A remarkable aspect of all radical species encountered in the meso compound is the fact that all hyperfine lines show an additional doublet splitting of 1.8 to 3.0 mT, probably due to proton splitting. The hyperfine coupling and **g** tensors of the three species labeled **2a**, **2b**, and **2c** are collected in Tables III and IV. The direction cosines in these tables are listed for only one of the four possible sites. The remaining three orientations are symmetry related to (x, y, z) via $(x, -y, -z)$, $(-x, y, -z)$, and $(-x, -y, z)$.

Radical **2a** is assigned to a three-electron-bond P–S radical (Figure 6). The estimated atomic orbital spin densities of the central phoshorus atom $\rho_{3s} = 10.3\%$ and $\rho_{3p} = 44.4\%$ are relatively close to the values found in recent studies on similar radicals generated in tetrasubstituted diphosphine disulfides and trialkylphosphine sulfides and selenides.[2,10] The isotropic hyperfine coupling (3s orbital contribution) of **2a** (1379 MHz) is somewhat smaller than that for these related species (1619–1776 MHz),

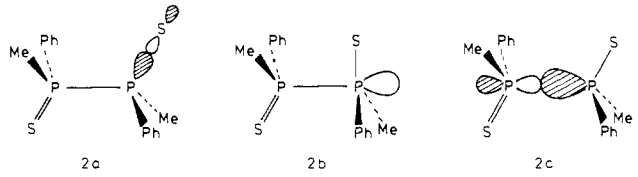

Figure 6. Structure of radicals **2a**, **2b**, and **2c**.

Table IV. g Tensors of Radicals **2a**, **2b**, and **2c**

radical	g	direction cosines		
		x	y	z
2a	1.997	0.784	0.460	−0.417
	2.010	−0.469	0.879	0.088
	2.025	0.407	0.126	0.905
2b	2.000	0.174	0.770	−0.614
	2.016	−0.428	0.621	0.657
	2.018	0.887	0.148	0.438
2c	1.981	0.380	0.787	−0.486
	2.010	−0.496	−0.271	0.825
	2.013	0.781	−0.555	0.287

whereas the dipolar interaction (3p orbital contribution) is larger (326 MHz vs 245–315 MHz). This results in an increased p/s ratio of 4.3 for **2a**, which is probably due to a small widening of the tetrahedral angle between the P–S bond and the bonds with the remaining three substituents.

Radical **2b** is characterized by a high isotropic phosphorus hyperfine coupling ($A^{iso} = 1934$ MHz, $\rho_{3s} = 14.4\%$) and a relatively small dipolar interaction ($B_{zz} = 186$ MHz, $\rho_{3p} = 25.3\%$) resulting in a p/s ratio of 1.8. Similar species have not been encountered so far in X-irradiated diphosphine disulfides. This complicates the identification of a radical structure for **2b**. The relatively low p/s ratio points to a trigonal-bipyramidal (TBP) radical structure, either with an equatorial (TBP-e) or an apical (TBP-a) location of the unpaired electron.[11-13] TBP-e structures, identified in tetramethyl- and tetraethyldiphosphine disulfides, exhibit hyperfine coupling to two phosphorus nuclei and their magnitudes are clearly different from those of **2b**.[2] We therefore propose a TBP-a like species with the SOMO pointing away from the substituents (Figure 6).

The third species, radical **2c**, exhibits hyperfine coupling to two distinct $I = {}^1/_2$ nuclei. The central phosphorus nucleus apparently bears a large amount of spin density since both the isotropic and anisotropic hyperfine couplings are very large, viz., $A^{iso} = 2316$ MHz and $B_{zz} = 373$ MHz. In fact these values are approximately two times the values of the symmetrical three-electron-bond radical **1a** in the racemate (vide supra). Nevertheless, the possibility that the large coupling is the result of the splitting between the $m_I = 1$ and $m_I = -1$ lines of a phosphorus triplet can be ruled out since the expected $m_I = 0$ transitions are absent. The weak absorptions in the $g = 2$ region of the ESR spectra of the meso form (Figure 4) are not related to the strong lateral absorptions because they are found to be much more persistent upon annealing the single crystal. A second possibility, that the large splitting is the result of a radical pair, one of whose components is a phosphoranyl type radical, seems unlikely because no transitions were observed in the half-field region between 70 and 260 mT. This leads to the conclusion that radical **2c** is a phosphorus centered radical, exhibiting a large hyperfine coupling to one ^{31}P nucleus and a small one to a second. The value of A^{iso} for the central phosphorus atom is appreciably larger than that for the other radicals encountered in X-irradiated diphosphine disulfides. We tentatively assign **2c** to a radical with an asymmetric three-electron P–P bond in which the unpaired electron is mainly localized on one of the two phosphorus nuclei (Figure 6). The spin density distribution, estimated from the hyperfine coupling parameters, amounts to

(10) Janssen, R. A. J.; Kingma, J. A. J. M.; Buck, H. M. *J. Am. Chem. Soc.* **1988**, *110*, 3018.

(11) Hasegawa, A.; Ohnishi, K.; Sogabe, K.; Miura, M. *Mol. Phys.* **1975**, *30*, 1367.

(12) Hamerlinck, J. H. H.; Schipper, P.; Buck, H. M. *J. Am. Chem. Soc.* **1980**, *98*, 7119.

(13) Howell, J. M.; Olsen, K. F. *J. Am. Chem. Soc.* **1976**, *98*, 7119.

Table V. Calculated Isotropic and Anisotropic Hyperfine Coupling Constants for *R,R* (C_2) and Meso (C_i) HMeP(S)P(S)MeH$^-$

radical	nucleus	A^{iso} au	A^{iso} MHz	B au	B MHz	direction cosines[a] x	y	z
R,R	P_1, P_2	0.602	1089	0.876	189	0.486	±0.049	0.873
				−0.402	−87	−0.022	±0.999	−0.044
				−0.474	−102	−0.874	±0.002	0.486
	S_1, S_2	0.011		0.811		0.170	±0.025	0.985
				−0.374		−0.069	±0.997	−0.013
				−0.437		−0.983	∓0.066	0.172
meso	P_1, P_2	0.602	1091	0.876	189	0.485	0.048	0.873
				−0.402	−87	−0.013	0.998	−0.048
				−0.474	−102	−0.874	0.012	0.485
	S_1, S_2	0.011		0.811		0.169	0.020	0.985
				−0.374		−0.068	0.998	−0.008
				−0.437		−0.983	−0.065	0.170

[a] Relative to the axis system in Figure 7.

ρ_{3s} = 17.3% and ρ_{3p} = 50.8% for the central atom, and ρ_{3s} = 1.0% and ρ_{3p} = 11.3% for the adjacent phosphorus nucleus. The directions of the dipolar hyperfine couplings of the two nuclei are inclined by an angle of 13° and therefore almost parallel, supporting the three-electron-bond assignment. Quantum chemical calculations have shown that the magnitude of A^{iso} in a three-electron-bond phosphoranyl radical can vary strongly with the angle between the three-electron bond and the remaining three substituents, possibly accounting for the large A^{iso} of the central phosphorus atom.[14]

The intensity of the ESR spectra of **2a**, **2b**, and **2c** decreases slowly upon annealing and the signals are irreversibly lost above 240 K.

Quantum Chemical Calculations

In this section we present a quantum chemical description of symmetrical three-electron-bond radicals in racemic and meso diphosphine disulfide radical anions. Since a full calculation on the two diastereoisomeric forms of the title compound would be very time consuming the calculations were restricted to (*R,R*)- and *meso*-1,2-dimethyldiphosphine disulfide, thereby replacing the phenyl groups by hydrogen atoms. Unrestricted Hartree–Fock (UHF) calculations were performed in order to obtain a theoretical geometry at which the hyperfine coupling parameters could be evaluated. Throughout the calculations a split valence 4-31G basis set[15,16] implemented with a single set of six second-order Gaussians on phosphorus and sulfur was used (radial exponents P 0.55, S 0.65).[17] The UHF procedure was followed by removal of the largest spin contaminant with use of the annihilation operator.[18]

The molecular geometry of the two diastereoisomeric radical anions was constrained to the point symmetry of the precursor molecules: C_2 for *R,R* and C_i for meso. Except for the CH bond lengths and the HCP bond angles which were simultaneously evaluated by using two variables, all molecular parameters were fully optimized in an analytical gradient procedure. This resulted in true energy minima for both the *R,R* and meso forms (Figure 7). Their structures are characterized by a relatively long P–P bond of 2.748 Å and a SPP bond angle of 142.2°. This elongation of the SPPS moiety is a direct result of the antibonding nature of the SOMO of these radicals. The isotropic and anisotropic (dipolar) hyperfine couplings were evaluated from the wave function by computing the expectation values of the corresponding operators.

$$A^{iso} = (8\pi/3)g\beta g_N\beta_N\langle\Psi_0|\delta(r_N)|\Psi_0\rangle$$

$$B_{ij} = -g\beta g_N\beta_N\left\langle\Psi_0\left|\frac{r^2\delta_{ij} - 3ij}{r^5}\right|\Psi_0\right\rangle$$

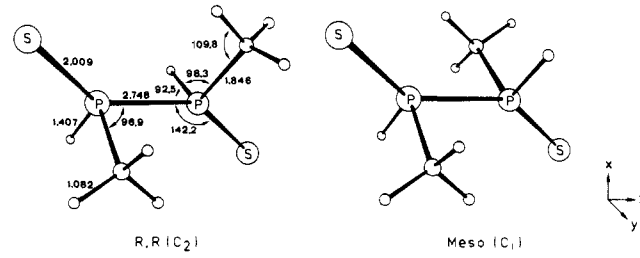

Figure 7. Optimized geometries for R,R (E(UHF) = −1555.242849 au, $\langle S^2\rangle$ = 0.7509) and meso (E(UHF) = −1555.242906 au, $\langle S^2\rangle$ = 0.7509) 1,2-dimethyldiphosphine disulfide three-electron bond radical anions.

After diagonalization of the B_{ij} matrix the three principal values are obtained, together with their directions relative to the molecular framework. The results of these calculations for the *R,R* and meso radical anions are compiled in Table V.

The hyperfine properties of the *R,R* 1,2-dimethyldiphosphine disulfide radical anion are in quantitative agreement with experiment. The two phosphorus nuclei hold most of the unpaired electron density. The value for A^{iso} is approximately 10% too small compared with radical **1a**, whereas the dipolar couplings deviate approximately 17% from experiment. The direction of the largest principal value of the dipolar hyperfine coupling, corresponding to the direction of the phosphorus 3p orbital contributing to the SOMO, makes an angle of 29.1° with the P–P bond. From the direction cosines in Table V it appears that the dipolar couplings of the two phosphorus nuclei are inclined by a small angle of 5.6°. This is a consequence of the C_2 symmetry of the *R,R* radical and indicates that the two phosphorus nuclei are not strictly magnetically equivalent for all orientations of a magnetic field.

Although the experiments do not reveal a symmetric three-electron-bond structure for the meso form, the calculations predict a stable geometry for the *meso*-1,2-dimethyldiphosphine disulfide radical anion. The hyperfine properties of this radical are very similar to the *R,R* couplings. However, by symmetry constraint (C_i) the principal directions of the dipolar couplings are now completely aligned and hence the phosphorus nuclei are magnetically equivalent.

Discussion

The present study reveals that there are major differences between the radicals generated in *rac-* and *meso*-1,2-dimethyl-1,2-diphenyldiphosphine disulfide. It is noteworthy that, besides a difference in the nature of the radical configurations, stronger ESR absorptions are found for the meso form than for the racemate, indicating a more efficient electron-capture process. There is no doubt that some variations in the radical configurations between racemate and meso could be expected in advance, because in principle the two diastereoisomers are different compounds. However, their difference is small since it concerns merely the stereochemistry around the phosphorus nuclei. The formation of a specific radical product is usually explained by taking into account the different properties of the substituents such as electronegativity. These arguments cannot be used to account for

(14) Janssen, R. A. J.; Visser, G. J.; Buck, H. M. *J. Am. Chem. Soc.* **1984**, *106*, 3429.
(15) Ditchfield, R.; Hehre, W. J.; Pople, J. A. *J. Chem. Phys.* **1971**, *4*, 724.
(16) Hehre, W. J.; Lathan, W. A. *J. Chem. Phys.* **1972**, *56*, 5255.
(17) Francl, M. M.; Pietro, W. J.; Hehre, W. J.; Binkley, J. S.; Gordon, M. S.; DeFrees, D. J.; Pople, J. A. *J. Chem. Phys.* **1982**, *77*, 3654.
(18) Amos, A. T.; Snyder, L. S. *J. Chem. Phys.* **1964**, *41*, 1773.

the present observations. The fact that no symmetrical three-electron-bond species are detected for the meso form can also not be explained by a possible wrong symmetry of the expected SOMO with respect to geometry of the parent molecule. In fact the *Ci* point symmetry fits excellently to a hypothetical symmetric antibonding orbital. This is confirmed by the quantum chemical calculations that predict stable geometries for both the racemic and meso form.

Apparently, the addition process of an extra electron to the diphosphine disulfides is able to discriminate between the several possible radical conigurations in a highly selective way. It is conceivable that the differentiation in the formation of the various electronic and geometric radical configurations is a consequence of the kinetics of the electron-capture process, rather than the result of (small) differences in total energy between the final radical products. In general electron-capture will lead to detectable electron-gain centers provided there is a relatively fast relaxation of the electron acceptor.[19] The relaxation may take the form of bond stretching or bending, or bond breaking, and it should lead to sufficiently deep traps to give detectable radical species. A possible explanation for the formation of a symmetric species in the racemate and asymmetric structures in the meso form can be obtained by assuming that the extra electron reacts with the parent molecules from a direction perpendicular to the plane of the phosphorus and sulfur nuclei. The electron will then first encounter one methyl and one phenyl group for the meso molecules and two methyl or two phenyl groups for the enantiomers *R,R* and *S,S*. Discrimination between a symmetric and an asymmetric radical product can then be rationalized by a difference in the rate of molecular relaxation (e.g., bond bending) in the solid state between the small methyl group and the large phenyl substituent. For the meso form the electron adds preferentially to the side of the methyl group rather than to the side with the phenyl substituent, resulting in an asymmetric radical configuration. For the molecules of the racemate (*R,R* and *S,S*), there is no difference between the relaxation rate of the two sides of the molecule and hence a symmetric electron-capture product is formed.

In the light of the present results further experimental and theoretical study on stereochemical selection in radical formation will be necessary.

Acknowledgment. This investigation has been supported by the Netherlands Foundation of Chemical Research (SON) with financial aid from the Netherlands Organization for the Advancement of Pure Research (ZWO). We thank G. C. Groenenboom for assistance in the quantum chemical calculations.

Registry No. 1, 13639-75-3; **1a**, 115181-91-4; **1b**, 115093-24-8; **2**, 13639-76-4; **2a**, 115181-92-5.

(19) Symons, M. C. R. *Pure Appl. Chem.* **1981**, *53*, 223.

Resonance Raman Studies of Dioxygen Adducts of Cobalt-Substituted Heme Proteins and Model Compounds. Vibrationally Coupled Dioxygen and the Issues of Multiple Structures and Distal Side Hydrogen Bonding

Alan Bruha and James R. Kincaid*

Contribution from the Chemistry Department, Marquette University, Milwaukee, Wisconsin 53233. *Received September 23, 1987*

Abstract: The resonance Raman (RR) spectra of the oxygen adducts of cobalt-substituted heme proteins have been carefully studied in the oxygen–oxygen stretching region. Included in the study are the cobalt analogues of myoglobin (Mb_{Co}), hemoglobin (Hb_{Co}), and its isolated subunits (α_{Co} and β_{Co}) as well as the iron/cobalt mixed hemoglobin hybrids, $(\alpha_{Co}\beta_{Fe})_2$ and $(\alpha_{Fe}\beta_{Co})_2$. The spectra of the $^{16}O_2$, $^{18}O_2$, and scrambled oxygen ($^{16}O_2$:^{16}O–^{18}O:$^{18}O_2$, 1:2:1) adducts have been measured in both normal (H_2O) and deuteriated (D_2O) buffers for each of the proteins. Strong bands located at ~1135, ~1098, and ~1065 cm^{-1} in H_2O solution are identified with $\nu(^{16}O–^{16}O)$, $\nu(^{16}O–^{18}O)$, and $\nu(^{18}O–^{18}O)$, respectively. Shifts of these bands in D_2O solution and the selective appearance of weaker features in the spectra of particular isotopic oxygen adducts are interpreted as the consequence of vibrational coupling of ν(O–O) with internal modes of the proximal and/or the distal histidylimidazole. The plausibility of this interpretation is supported by the observation of similar behavior in model compound systems which is documented here and in earlier studies. All of the major and minor features observed in the spectra of the proteins can be explained without requiring the existence of two liganded (O_2) conformers, in contrast to earlier interpretations. In addition, based on the results of model compound studies, the frequency observed for ν(O–O) indicates that the bound dioxygen is hydrogen bonded to the distal histidylimidazole in these protein systems. However, the present interpretation argues that the frequency shifts of $\nu(^{16}O–^{16}O)$ observed upon replacement of H_2O by D_2O cannot be taken as evidence for this distal side hydrogen bonding. Finally, it is suggested that the spectroscopic consequences of such coupling not only complicate the interpretation of oxygen adduct spectra but also (in a positive light) may provide a powerful spectroscopic probe of subtle structural perturbations once they are more fully understood and properly calibrated.

The oxygen transport proteins, hemoglobin (Hb) and myoglobin (Mb), are perhaps the most thoroughly studied of all biomolecules.[1] Despite intensive effort by many research groups and an extensive body of accumulated knowledge, questions remain unanswered, even at a rather fundamental level. In fact, knowledge of the details of O_2 structure and bonding at the heme site remains incomplete. Thus, issues such as the importance of distal side hydrogen bonding between the bound O_2 and the heme pocket distal histidine[2-7] and even the number of stable structures[7-9] remain controversial.

(1) *Hemoglobins*; Antonini, E., Rossi-Bernardi, L., Chiancone, E., Eds.; Academic Press: New York, 1981; Vol. 76.

(2) Mims, M. P.; Porras, A. G.; Olsen, J. S.; Noble, R. W.; Peterson, J. A. *J. Biol. Chem.* **1983**, *258*, 14219.
(3) Pauling, L. *Nature (London)* **1964**, *203*, 182.
(4) Phillips, S. E. V.; Schoenborn, B. P. *Nature (London)* **1981**, *292*, 81.
(5) Shaanan, B. *Nature (London)* **1982**, *296*, 683.
(6) Shaanan, B. *J. Mol. Biol.* **1983**, *171*, 31.
(7) Phillips, S. E. V. *J. Mol. Biol.* **1980**, *142*, 531.
(8) Potter, W. T.; Tucker, M. P.; Houtchens, R. A.; Caughey, W. S. *Biochemistry* **1987**, *26*, 4699.

0002-7863/88/1510-6006$01.50/0